

# Statin-Induced Cancer Cell Death Can Be Mechanistically Uncoupled from Prenylation of RAS Family Proteins

Rosemary Yu<sup>1,2</sup>, Joseph Longo<sup>1,2</sup>, Jenna E. van Leeuwen<sup>1,2</sup>, Peter J. Mullen<sup>1</sup>, Wail Ba-Alawi<sup>1</sup>, Benjamin Haibe-Kains<sup>1,2,3,4</sup>, and Linda Z. Penn<sup>1,2</sup>



## Abstract

The statin family of drugs preferentially triggers tumor cell apoptosis by depleting mevalonate pathway metabolites farnesyl pyrophosphate (FPP) and geranylgeranyl pyrophosphate (GGPP), which are used for protein prenylation, including the oncoproteins of the RAS superfamily. However, accumulating data indicate that activation of the RAS superfamily are poor biomarkers of statin sensitivity, and the mechanism of statin-induced tumor-specific apoptosis remains unclear. Here we demonstrate that cancer cell death triggered by statins can be uncoupled from prenylation of the RAS superfamily of oncoproteins. Ectopic expression of different members of the RAS superfamily did not uniformly sensitize cells to fluvastatin, indicating that increased cellular demand for protein prenylation cannot explain increased statin sensitivity. Although ectopic expression of HRAS increased statin sensitivity, expression of myristoylated

HRAS did not rescue this effect. HRAS-induced epithelial-to-mesenchymal transition (EMT) through activation of zinc finger E-box binding homeobox 1 (ZEB1) sensitized tumor cells to the antiproliferative activity of statins, and induction of EMT by ZEB1 was sufficient to phenocopy the increase in fluvastatin sensitivity; knocking out ZEB1 reversed this effect. Publicly available gene expression and statin sensitivity data indicated that enrichment of EMT features was associated with increased sensitivity to statins in a large panel of cancer cell lines across multiple cancer types. These results indicate that the anticancer effect of statins is independent from prenylation of RAS family proteins and is associated with a cancer cell EMT phenotype.

**Significance:** The use of statins to target cancer cell EMT may be useful as a therapy to block cancer progression. *Cancer Res*; 78(5); 1347–57. ©2017 AACR.

## Introduction

Statins are inhibitors of 3-hydroxy-3-methylglutaryl coenzyme A reductase (HMGCR; Fig. 1A), and have been widely prescribed to lower cholesterol levels (1). Epidemiologic evidence indicate that statins have anticancer activities, particularly in breast and prostate cancers (2–5). Preclinical and clinical data demonstrate that statin treatment induces cancer cells to undergo apoptosis and lowers disease burden (6–9). Despite the promising potential to repurpose statins as anticancer agents, the molecular mechanism of how inhibition of HMGCR can specifically kill cancer cells remains unclear.

HMGCR catalyzes the conversion of HMG-CoA to mevalonate (MVA), the sole precursor for the *de novo* synthesis of sterols, geranylgeranyl pyrophosphate (GGPP), farnesyl pyrophosphate (FPP), and several other metabolic endproducts (Fig. 1A; refs.

1, 10). Statin-induced apoptosis can be rescued by coadministration with MVA (8, 11), demonstrating that this is an on-target effect, or with GGPP or FPP (8, 11–15). Sterols cannot rescue cancer cell apoptosis induced by statins (8). These results have led to a model where statins induce apoptosis by inhibiting GGPP and FPP synthesis.

GGPP and FPP are essential substrates for protein geranylgeranylation and farnesylation, respectively, together referred to as protein prenylation (16). Prenylation with the hydrophobic geranylgeranyl or farnesyl moiety localizes proteins to cellular membranes (16). Prenylation-driven membrane localization is required for all proteins in the RAS GTPase superfamily, and several groups have shown that statin treatment decreases the prenylated and membrane-associated forms of RAS, RHO, RAC, RAP, and RAB subfamily proteins (12, 17–20). However, evidence for the functional importance of these small GTPases in conferring statin sensitivity has been conflicting. For example, cancer cells with upregulated or hyperactivated RAS or RHO demonstrate increased statin sensitivity in some studies (17–19), but not others (8, 14, 21). Understanding the mechanism driving these discrepancies has remained a challenge and has been an area of debate for many years (10).

In this manuscript, we directly address these discrepancies and show that inhibition of RAS family protein prenylation is not essential for, and can be uncoupled from, statin-induced cell death. We chose MCF10A cells as our model system as they are an immortal, nontransformed basal breast cell line that possesses a highly stable genome, allowing for the evaluation of ectopic gene expression in the absence of gross genetic instability (22). We

<sup>1</sup>Princess Margaret Cancer Centre, University Health Network, Toronto, Ontario, Canada. <sup>2</sup>Department of Medical Biophysics, University of Toronto, Toronto, Ontario, Canada. <sup>3</sup>Department of Computer Science, University of Toronto, Toronto, Ontario, Canada. <sup>4</sup>Ontario Institute of Cancer Research, Toronto, Ontario, Canada.

**Note:** Supplementary data for this article are available at Cancer Research Online (<http://cancerres.aacrjournals.org/>).

**Corresponding Author:** Linda Z. Penn, Princess Margaret Cancer Centre, 13th Floor 13-706, 101 College St., Toronto, Ontario M5G 1L7, Canada. Phone: 416-634-8770; E-mail: Linda.Penn@uhnresearch.ca

**doi:** 10.1158/0008-5472.CAN-17-1231

©2017 American Association for Cancer Research.

systematically introduced several members of the RAS superfamily in the MCF10A cell line to produce a panel of sublines with increased demand for GGPP and/or FPP. This did not uniformly sensitize cells to inhibition of GGPP and FPP synthesis, as only HRAS<sup>G12V</sup> and KRAS<sup>G12V</sup> exhibited an increased sensitivity to fluvastatin. HRAS<sup>G12V</sup> and myristoylated-HRAS<sup>G12V</sup> sensitized cells to statins to a similar extent, indicating that statin-induced cell death is independent of RAS prenylation, even in RAS-transformed cells. We then showed that overexpression of RAS induced epithelial-to-mesenchymal transition (EMT) in these cells, in part by upregulating the EMT driver zinc finger E-box binding homeobox 1 (ZEB1). Exogenous expression or knockout of ZEB1 conferred or rescued statin sensitivity, respectively, suggesting that EMT was the critical feature that was functionally important for statin-induced cell death. Taking a computational pharmacogenomics approach, we discovered that EMT was associated with statin sensitivity across a large panel of cancer cell lines. Taken together, our results provide a rationale for why RAS-related oncogenes have been poor biomarkers of statin sensitivity, and suggest that a set of EMT-associated genes should be further evaluated in the preclinical and clinical setting as biomarkers of statin sensitivity.

## Materials and Methods

### Reagents

Fluvastatin and TGF $\beta$  were purchased from US Biologicals and PeproTech, respectively. Other chemicals were purchased from Sigma unless otherwise specified.

### Cell culture

MCF10A cells were a kind gift of Dr. Senthil Muthuswamy; MGH8, H1264, and RVH6849 were kind gifts of Dr. Ming Tsao; Mia-Paca-2 was a kind gift of Dr. David Hedley; KP-4 was a kind gift of Dr. Bradley Wouters; and HT-29 was a kind gift of Dr. Catherine O'Brien. All cell lines were cultured as recommended by ATCC. All cell lines were authenticated by short-tandem repeat (STR) profiling, and routinely tested to be free of mycoplasma by Lonza MycoAlert Mycoplasma Detection Kit. All cell lines were used within 20 passages from thawing for the described experiments. Transgene expression was stably introduced into MCF10A cells using retroviral insertion with pBabe-Puro. Cells were imaged on the Leica MZ FLIII Stereomicroscope.

### MTT assays

3-(4,5-Dimethylthiazol-2-yl)-2,5-diphenyltetrazolium bromide (MTT) assays were performed as previously described (6). Briefly, MCF10A cells were seeded at 750 cells/well in 96-well plates overnight, then treated in triplicate with 0 to 200  $\mu$ mol/L fluvastatin for 72 hours. IC<sub>50</sub> values were computed using Graph-Pad Prism with a bottom constraint equal to 0.

### Immunoblotting

Cell lysates were prepared by lysing directly in boiling SDS lysis buffer (1% SDS, 11% glycerol, 10%  $\beta$ -mercaptoethanol, 0.1 mol/L Tris pH 6.8). The following antibodies were used: E-Cadherin (CST 3195), vimentin (CST 5741), actin (Sigma A2066), tubulin (Millipore CP06), FLAG (Sigma F1804), EGFR (CST 2232), ERK (CST 4695), p-ERK (CST 4370), AKT (CST 9272), p-AKT (CST 9271), HMGCS1 (SCB sc-32423), RALA (BD 610221), BRAF (Sigma HPA001328), MYC (Mab 9E10 prepared in-house using ATCC CRL-1729), ZEB1 (Sigma

HPA027524), HMGCR (Mab A9 prepared in-house using ATCC CRL-1811).

### Soft agar colony formation

Anchorage-independent colony growth of MCF10A sublines in soft agar was evaluated as previously described (23). Colonies were imaged at 1.2 $\times$  magnification on the Leica MZ FLIII Stereomicroscope after 14 to 18 days of fluvastatin treatment. Colony number and average colony size were quantified using ImageJ.

### Membrane fractionation

Cell were seeded at  $2 \times 10^6$ /plate overnight and treated as indicated. Harvested cells were resuspended in 1 mL HEPES buffer (0.25 mol/L sucrose, 50 mmol/L HEPES pH 7.5, 5 mmol/L NaF, 5 mmol/L EDTA, 2 mmol/L DTT) and lysed by sonication. Homogenate was cleared at  $2,000 \times g$  for 20 minutes at 4°C, then ultracentrifuged at  $115,000 \times g$  for 70 min at 4°C for membrane fractionation. Membrane protein pellet was resuspended in Triton buffer (1% TritonX-114, 50 mmol/L Tris pH 7.5, 0.1 mmol/L NaCl, 5 mmol/L EDTA, 5 mmol/L NaF, 2 mmol/L DTT).

### Cell death assay

Cells were seeded at  $2.5 \times 10^5$ /plate overnight and treated as indicated. After 72 hours, cells were fixed in 70% ethanol for >24 hours, stained with propidium iodide, and analyzed by flow cytometry for the % sub-diploid DNA population as % cell death, as previously described (6).

### qRT-PCR

Total RNA was harvested from subconfluent cells using TRIzol Reagent (Invitrogen). cDNA was synthesized from 500 ng of RNA using SuperScript III (Invitrogen). Real-time quantitative RT-PCR was performed using TaqMan probes for HMGCR (ABI Hs00168352), HMGCS1 (ABI Hs00266810), and GAPDH (ABI Hs99999905), and using SYBR Green for TWIST, SNAIL, ZEB1, and 18S rRNA with the following primers:

TWIST\_fw 5'-CCGGAGACCTAGATGTCATTG-3'  
 TWIST\_rv 5'-CCACGCCCTGTTTCITTTG-3'  
 SNAIL\_fw 5'-CACTATGCCGCGCTCTTTC-3'  
 SNAIL\_rv 3'-GGTCGTAGGGCTGCTGGAA-3'  
 ZEB1\_fw 5'-GCCAATAAGCAAACGATTCTG-3'  
 ZEB1\_rv 5'-TTTGCTGGATCACTTCAAG-3'  
 18S\_rRNA\_fw 5'-GTAACCCGTTGAACCCCAT-3'  
 18S\_rRNA\_rv 3'-CCATCCAATCGGTAGTAGCG-3'

### CRISPR/Cas9-mediated gene knockout

Two sgRNAs were designed using CRISPOR (24) and cloned into LentiGuide-Puro following the established protocol (25). ZEB1 knockout lines were generated as previously described (25). LentiGuide-Puro (Addgene #52963) and LentiCas9-Blast (Addgene #52962) were kind gifts from Dr. Feng Zhang (Broad Institute of MIT and Harvard, Cambridge, MA). Sequences of ZEB1 sgRNAs cloned were:

sgRNA A: TGCTTTCTGCGCTTACACCT GGG  
 sgRNA B: GCAGAAAGCAGCGCAACCCG CGG

### Pharmacogenomic analysis

RNA-seq and drug sensitivity data were retrieved and curated from the Cancer Cell Line Encyclopedia (CCLE; ref. 26) and the

Cancer Therapeutics Portal version 2 (CTRPv2; refs. 27–29) databases, and were mined using the R/Bioconductor PharmacoGx package (30). To calculate the bimodality index (31, 32), a mixture of two Gaussian models was used to fit the RNA-seq expression values of each gene across all cell lines in CCLE, as implemented in the bimod function in the R/Bioconductor genefu package (version 2.6.0; ref. 32). The cutoff was calculated by finding the midpoint between the maximum value of the first Gaussian model (left distribution) and the minimum value of the second Gaussian model (right distribution). The cutoff was used to classify cell lines into either showing low or high expression of a gene. A binary classification rule was developed to determine whether a cell line is "enriched" with EMT phenotype or not. Cell lines from tumors of hematopoietic and lymphoid tissues, and those with unknown origin, were excluded from this analysis. If expression of any of *VIM*, *ZEB1*, *FN1*, or *CDH2* was high, or if expression of *CDH1* was low, in a cell line according to the bimodality cutoff, then it was classified as "enriched" with EMT phenotype. Concordance index (CI) and *P*-value were calculated to measure the association between statin sensitivity, obtained from CTRPv2 database, and cell lines that were classified as either "enriched" with EMT phenotype or "not enriched." *P*-value was calculated using the nonparametric Wilcoxon rank sum test, comparing statin response on cell lines "enriched" versus "not enriched" with the EMT phenotype. The script and data used for the generation of these figures can be downloaded at <https://github.com/bhklab/StatinEMT>.

## Results

### HRAS<sup>G12V</sup> and KRAS<sup>G12V</sup>, but not other proteins in the RAS superfamily, sensitize MCF10A cells to fluvastatin

Using the MCF10A breast epithelial cell line as a nontransformed, genomically stable cell background (22), we ectopically expressed representative proteins from the RAS, RHO, RAC, and RAP subfamilies in their dominantly active forms (Fig. 1B; ref. 16). These mutants remain dependent on prenylation for activity, allowing us to simulate an increase in demand for FPP and/or GGPP as a result of aberrant activation of these GTPases. The increase in demand for FPP and/or GGPP did not universally sensitize cells to fluvastatin (Fig. 1C), as only cells overexpressing HRAS<sup>G12V</sup> or KRAS<sup>G12V</sup> had significantly lowered fluvastatin IC<sub>50</sub> values (13.6 and 13.2 μmol/L, respectively) compared to the vector control (22.2 μmol/L), which indicated an increased sensitivity to fluvastatin (Fig. 1C). A colony formation assay in soft agar was used to test the inhibitory effect of fluvastatin treatment on the transformation potential of these cells (Fig. 1D; Supplementary Fig. S1A). In this and all subsequent colony formation assays, 20 μmol/L fluvastatin was used to allow for adequate penetrance into the soft agar. Fluvastatin treatment significantly reduced both colony count (Fig. 1E) and colony size (Fig. 1F) of cells overexpressing HRAS<sup>G12V</sup> and KRAS<sup>G12V</sup>, but not those expressing other proteins in the RAS superfamily (Supplementary Fig. S1B–S1D). Thus, compared to other members of the RAS superfamily, activated HRAS and KRAS preferentially sensitize MCF10A cells to the anticancer activity of fluvastatin.

### Inhibition of RAS prenylation is uncoupled from fluvastatin-induced cell death

If inhibition of RAS localization was the mechanism of fluvastatin-induced cell death, cells overexpressing myristoylated

HRAS<sup>G12V</sup> (myr-HRAS), which localizes to the cell membrane independently of prenylation with FPP or GGPP, should remain insensitive to fluvastatin. Figure 2A shows that overexpression of HRAS<sup>G12V</sup> and myristoylated HRAS<sup>G12V</sup> both activated downstream signaling to a similar extent, as seen by the increase in Erk and Akt phosphorylation. Although the mislocalization of HRAS<sup>G12V</sup> from the membrane to the cytoplasm was evident after treatment with 10 μmol/L of fluvastatin for 24 hours, myr-HRAS<sup>G12V</sup> remained in the membrane fraction, confirming that myristoylation occurs independent of FPP and GGPP (Fig. 2B). EGFR, HMGCS1, and actin were used as controls for membrane-localized, cytosol-localized, and total proteins, respectively (Fig. 2B). Unexpectedly, the fluvastatin IC<sub>50</sub> value of cells overexpressing myr-HRAS<sup>G12V</sup> was significantly decreased similarly to HRAS<sup>G12V</sup> (Fig. 2C). Colony formation was also inhibited by fluvastatin treatment in cells overexpressing myr-HRAS<sup>G12V</sup> (Fig. 2D–F), to the same extent as cells overexpressing HRAS<sup>G12V</sup> (Fig. 1D–F). Addition of MVA, GGPP, or FPP rescued the fluvastatin-induced cell death in both HRAS<sup>G12V</sup> and myr-HRAS<sup>G12V</sup> cells (Fig. 2G–I). Together, these data uncouple statin-induced cell death from GGPP and FPP demand for prenylation of RAS family proteins, and implicate that events downstream of RAS signaling are responsible for the increase in statin sensitivity in this cell system.

### The RAS–ZEB1–EMT signaling axis underlies increased sensitivity to fluvastatin

We next addressed several potential models to understand the mechanism of RAS sensitization of MCF10A cells to the antiproliferative activity of fluvastatin. Overexpression of HRAS<sup>G12V</sup> or myr-HRAS<sup>G12V</sup> in MCF10A cells did not affect the expression of MVA pathway genes HMGCR and HMGCS1, either basally or in response to fluvastatin exposure (Supplementary Fig. S2A and S2B). This rules out impairment of the sterol feedback response as the mechanism of increased statin sensitivity in this model, which were previously reported to be associated with statin sensitivity in multiple myeloma (6).

Because RAS signaling, rather than RAS localization, was implicated as the driver of fluvastatin sensitivity, we overexpressed constitutively active forms of several classic effectors of RAS signaling (RALA<sup>G23V</sup>, BRAF<sup>V600E</sup>, PI3K-p110α<sup>E545K</sup>, PI3K-p110α<sup>H1047R</sup>, and MYC<sup>T58A</sup>), to determine which of these, if any, phenocopied the increase in fluvastatin sensitivity in RAS-overexpressing cells. None of these sublines exhibited a lowered fluvastatin IC<sub>50</sub> (Supplementary Fig. S3A–S3C). By contrast, overexpression of PI3K-p110α led to significant increases in IC<sub>50</sub> values (Supplementary Fig. S3A–S3C). Similar results were evident in soft agar colony formation assays (Supplementary Fig. S3D–S3F). Therefore, the observed increase in fluvastatin sensitivity in RAS-transformed cells was not mediated through these downstream mediators of RAS signaling.

The RAS sublines were phenotypically distinct from the MCF10A parental cells. Instead of an epithelial phenotype with a cobblestone-like appearance, the RAS sublines appeared more mesenchymal, with an elongated and spindle-shaped morphology (Fig. 3A). These cells had undergone EMT, with a dramatic loss of E-cadherin expression and a gain of vimentin expression (Fig. 3B). By contrast, sublines overexpressing other members of the RAS superfamily (Supplementary Fig. S1D) and classic effectors of RAS signaling (Supplementary Fig. S3C) remained

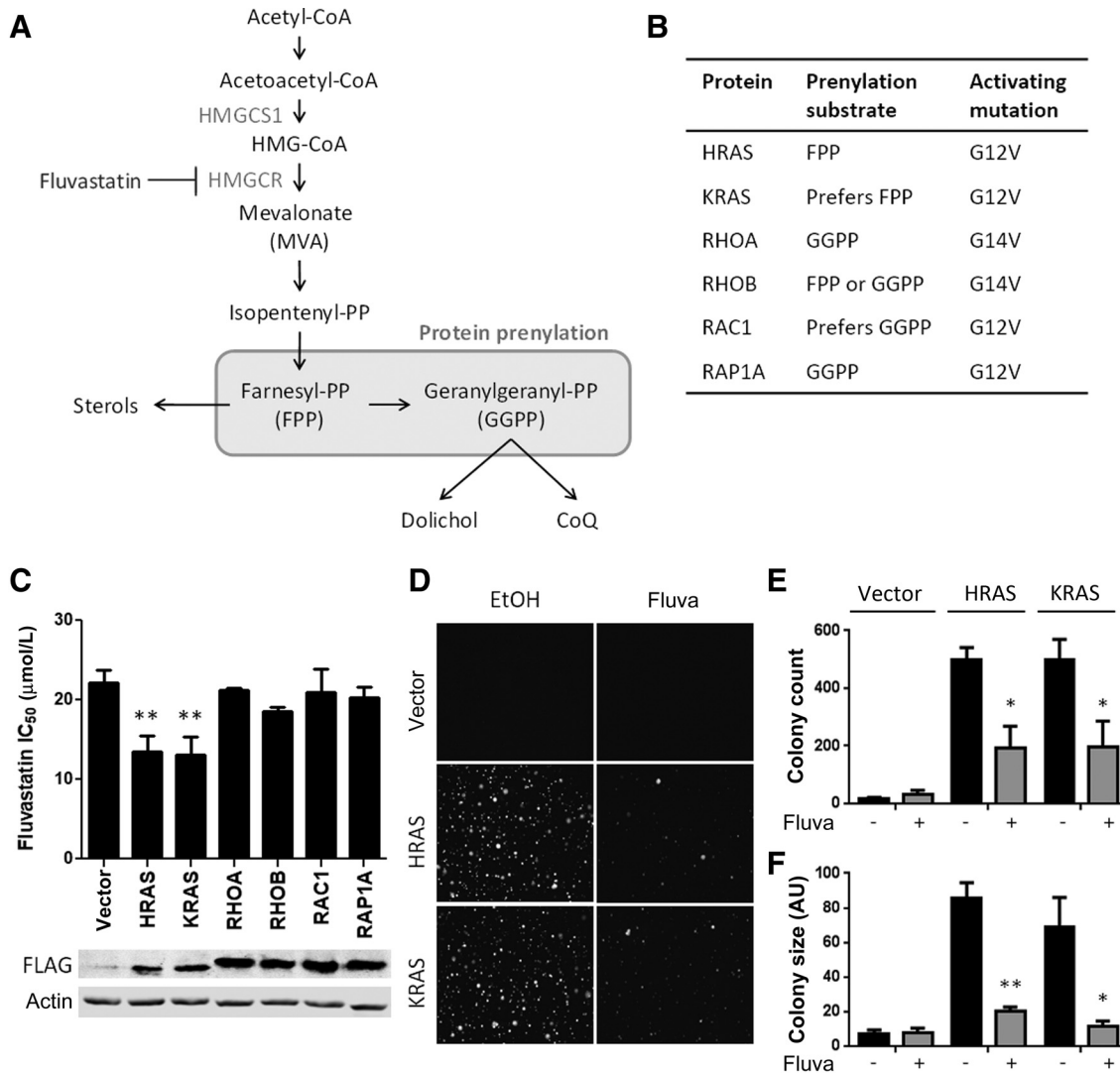


**Figure 1.** HRAS<sup>G12V</sup> and KRAS<sup>G12V</sup>, but not other prenylated proteins, sensitize MCF10A cells to fluvastatin. **A**, A simplified schematic of the MVA pathway. **B**, Representative RAS family proteins selected for ectopic expression in MCF10A cell lines. **C**, Ectopic expression of HRAS<sup>G12V</sup> and KRAS<sup>G12V</sup> sensitized MCF10A cells to fluvastatin, as assessed by MTT assay following 72 hours of treatment. Bars, mean + SD, *n* = 3. \*\*, *P* < 0.01 (one-way ANOVA with a Dunnett posttest, comparing all columns vs. vector control column). **D–F**, Treatment with fluvastatin decreased colony count and colony size of RAS-driven anchorage-independent growth in soft agar. Colonies were treated with 20 μmol/L fluvastatin 2× weekly for 18 days. Bars, mean + SD, *n* = 4. \*, *P* < 0.05; \*\*, *P* < 0.01 (unpaired, two-tailed *t* test, comparing fluvastatin-treated vs. no treatment control).

epithelial, expressing E-cadherin and vimentin at similar levels to the vector controls. To test whether induction of EMT confers sensitivity to fluvastatin, we treated MCF10A cells with TGFβ for 3 days, which induces EMT independently of RAS status (Fig. 3C). This led to an increased sensitivity to fluvastatin, as indicated by a decrease in fluvastatin IC<sub>50</sub> in TGFβ-treated cells (Fig. 3D). After TGFβ treatment, removal of TGFβ from the culture media gradually reverses EMT (Supplementary Fig. S4). MCF10A cells fully reverted back to an epithelial phenotype 7 days after the removal of TGFβ, and sensitivity to fluvastatin was restored to control levels (Supplementary Fig. S4). These data indicate that a mesenchymal state is sufficient to confer sensitivity to fluvastatin.

RAS induces EMT by upregulating the EMT-driving transcription factor ZEB1, and not by other EMT regulators such as SNAIL or TWIST in our MCF10A system (Fig. 3E). ZEB1-overexpression in MCF10As led to a loss of E-cadherin and gain of vimentin expression independent of RAS status (Fig. 3F), and decreased the fluvastatin IC<sub>50</sub> value similarly to the RAS sublines (Fig. 3G). ZEB1 overexpression had no effect on the IC<sub>50</sub> value of GGTI-298 (Fig. 3H), a specific inhibitor to geranylgeranyltransferase I, reinforcing the model that prenylation of RAS family proteins is uncoupled from fluvastatin-induced tumor cell death. We then knocked out ZEB1 in cells with ectopic expression of HRAS<sup>G12V</sup> and myr-HRAS<sup>G12V</sup>, and showed that ZEB1 knockout reversed cells to epithelial state, as evidenced by

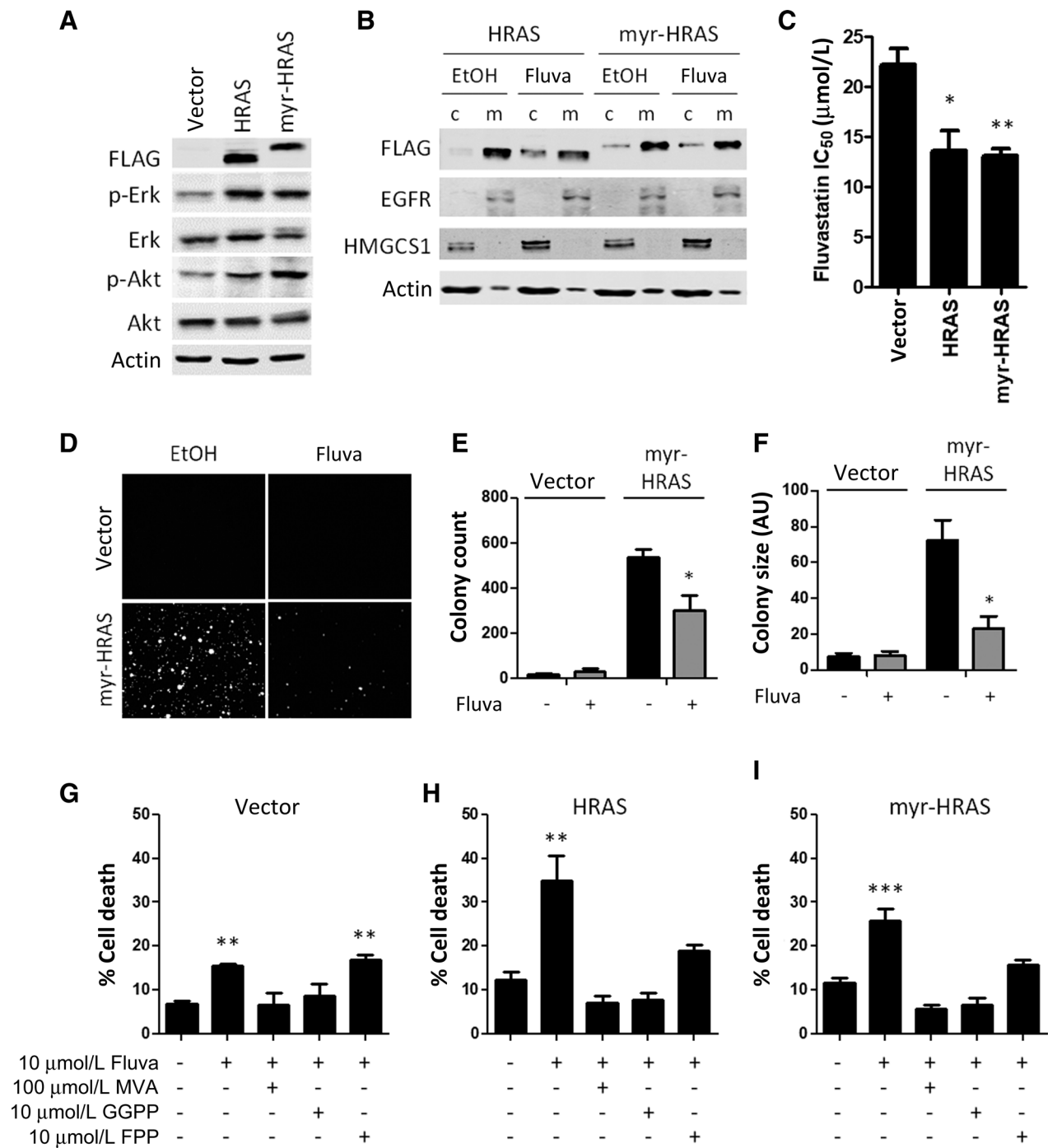


**Figure 2.** Inhibition of RAS prenylation is uncoupled from fluvastatin-induced cell death. **A**, Overexpression of HRAS<sup>G12V</sup> and myr-HRAS<sup>G12V</sup> activated Erk phosphorylation and Akt phosphorylation to a similar extent. **B**, The proportion of HRAS<sup>G12V</sup> in the cytoplasmic (c) fraction was increased, and the proportion in the membrane (m) proportion was decreased after 24 hours of treatment with 10 μmol/L fluvastatin. In contrast, the localization of myr-HRAS<sup>G12V</sup> was unaffected by fluvastatin treatment. **C**, Both HRAS<sup>G12V</sup> and myr-HRAS<sup>G12V</sup> sensitized MCF10As to fluvastatin as assessed by MTT assay following 72 hours of treatment. Bars, mean + SD, *n* = 3. \*, *P* < 0.05; \*\*, *P* < 0.01 (one-way ANOVA with a Dunnett posttest, comparing all columns vs. vector control column). **D–F**, Treatment with fluvastatin decreased colony count and colony size of myr-HRAS<sup>G12V</sup>-driven anchorage-independent growth in soft agar. Colonies were treated with 20 μmol/L fluvastatin 2× weekly for 18 days. Bars, mean + SD, *n* = 4. \*, *P* < 0.05 (unpaired, two-tailed *t* test, comparing fluvastatin-treated vs. no treatment control). **G–I**, Ten μmol/L fluvastatin induced cell death in MCF10A cells overexpressing HRAS<sup>G12V</sup> and myr-HRAS<sup>G12V</sup>, which was reversed by coadministration with MVA, GGPP, or FPP. Bars, mean + SD, *n* = 3. \*\*, *P* < 0.01; \*\*\*, *P* < 0.001 (one-way ANOVA with a Dunnett posttest, comparing all columns vs. no treatment control column).

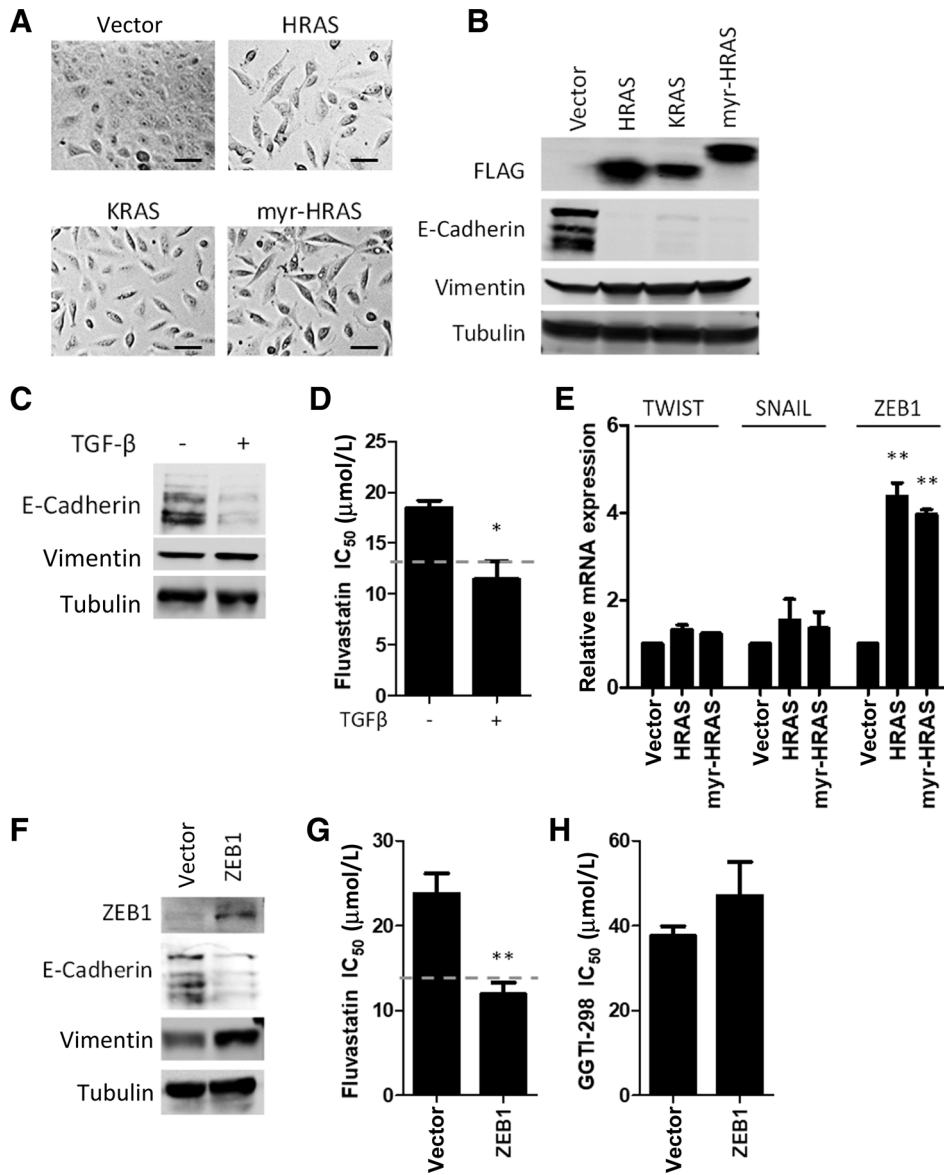


**Figure 3.** RAS induces EMT through ZEB1, and induction of EMT is sufficient for sensitizing cells to fluvastatin. **A**, RAS-overexpressing cells appear more mesenchymal than the vector control cells. Representative images are shown. Scale bar, 50  $\mu\text{m}$ . **B**, RAS overexpression reduced expression of E-cadherin, an epithelial cell marker, and increased expression of vimentin, a mesenchymal cell marker. **C**, Treating MCF10A cells with 5 ng/mL TGF $\beta$  for 3 days induced EMT. **D**, Induction of EMT by 5 ng/mL TGF $\beta$  treatment sensitized MCF10A cells to fluvastatin, as assessed by MTT assay following 72 hours of treatment. Dashed line represents IC<sub>50</sub> of HRAS<sup>G12V</sup>-overexpressing cells. Bars, mean + SD,  $n = 3$ . \*,  $P < 0.05$  (unpaired, two-tailed  $t$  test, comparing TGF $\beta$ -treated vs. no treatment control). **E**, HRAS<sup>G12V</sup> and myr-HRAS<sup>G12V</sup> cells upregulate the EMT transcription factor ZEB1. Bars, mean + SD,  $n = 3$ . \*\*,  $P < 0.01$  (one-way ANOVA with a Dunnett posttest, comparing all columns vs. vector control column). **F**, Ectopic expression of ZEB1 induced EMT. **G**, ZEB1 overexpression sensitized MCF10A cells to fluvastatin, as assessed by MTT assay following 72 hours of treatment. Dashed line represents IC<sub>50</sub> of HRAS<sup>G12V</sup>-overexpressing cells. Bars, mean + SD,  $n = 3$ . \*\*,  $P < 0.01$  (unpaired, two-tailed  $t$  test, comparing TGF $\beta$ -treated vs. no treatment control). **H**, ZEB1 overexpression did not sensitize cells to GGTI-298. Bars, mean + SD,  $n = 3$ .

the increased expression of E-cadherin and decreased expression of vimentin (Fig. 4A). Knocking out ZEB1 rescued the RAS-driven fluvastatin sensitivity, both by IC<sub>50</sub> measurements (Fig. 4B) and by colony formation in soft agar (Fig. 4C–E).

**Enrichment of EMT phenotype is associated with sensitivity to statins in a large panel of cancer cell lines**

The CCLE database (26) contains RNA-seq data of 927 cancer cell lines across >20 cancer types (Supplementary Fig. S5A). Mining this large database, we observed that although the expression pattern for most genes follow a unimodal (Gaussian) distribution, as exemplified by *POLR2A* (RNA polymerase II, subunit A; Fig. 5A), some genes are bimodally expressed, such as *ESR1* (estrogen receptor  $\alpha$ ; Fig. 5A; Supplementary Fig. S5B). *ESR1* is known for a strong bimodal expression in breast tissue (32, 33), representing ER $\alpha$ -low (left peak) and ER $\alpha$ -high (right peak) cell lines (Fig. 5A; Supplementary Fig. S5B). We then examined the

expression profile of 11 well-characterized EMT-associated genes, and observed that their expression were strongly bimodal, with bimodality indices (31, 32) higher than that of *ESR1*, our positive control (Supplementary Fig. S5C). The distribution of the top five bimodally expressed genes (*VIM*, *CDH1*, *ZEB1*, *FN1*, and *CDH2*) is shown in Fig. 5A. For each gene, we computed the cutoff optimally discriminating between the two modes of expression distribution, and classified the cell lines with either low or high expression of the gene of interest (Fig. 5A). Each cell line was therefore characterized by a binary vector representing the activation of the top five bimodally expressed EMT-associated genes.

Using the top five bimodally expressed EMT-associated genes as features, we built a binary classification rule that classified each solid tumor cell line as enriched with an EMT phenotype if at least one of the EMT-associated genes was activated (Fig. 5A, right peak for *VIM*, *ZEB1*, *FN1*, and *CDH2*; left peak for *CDH1*). We then mined the CTRPv2 database (27–29) using the PharmacoGx R/

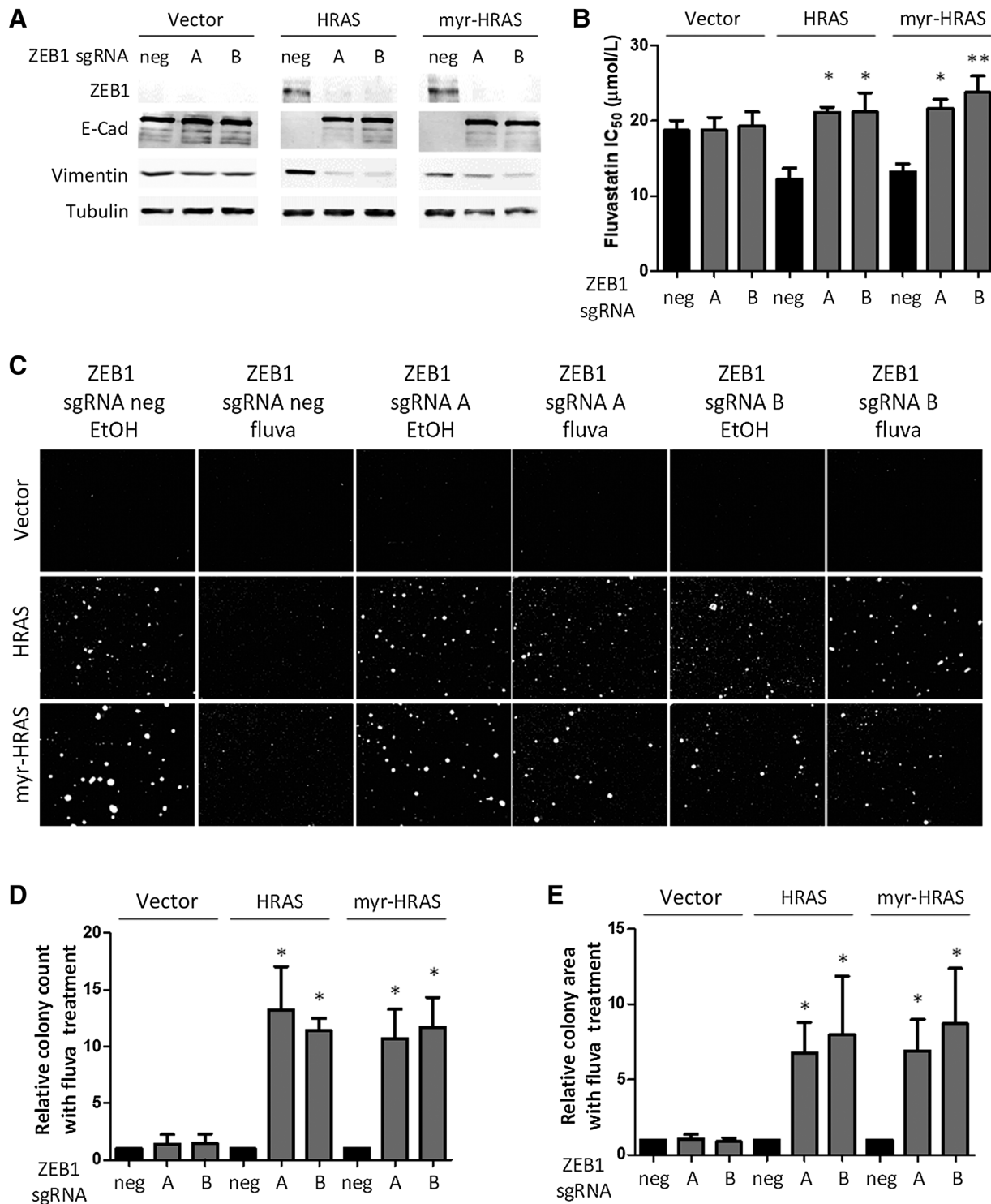


**Figure 4.** CRISPR/Cas9-mediated knockout of ZEB1 reverses EMT and rescues the increased sensitivity in HRAS<sup>G12V</sup> and myr-HRAS<sup>G12V</sup> cells. **A**, Two independent sgRNAs (**A** and **B**) were used to knockout ZEB1 in MCF10A cells overexpressing HRAS<sup>G12V</sup> and myr-HRAS<sup>G12V</sup>. Knocking out ZEB1 reversed cells to epithelial state, as seen by the increased expression of E-cadherin and decreased expression of vimentin. **B**, ZEB1 knockout rescued the decreased fluvastatin IC<sub>50</sub> observed in HRAS<sup>G12V</sup> and myr-HRAS<sup>G12V</sup> cells. Bars, mean + SD,  $n = 3$ . \*,  $P < 0.05$ ; \*\*,  $P < 0.01$  (one-way ANOVA with a Dunnett posttest, comparing all columns vs. vector control column). **C-E**, ZEB1 knockout in HRAS<sup>G12V</sup> and myr-HRAS<sup>G12V</sup> cells led to increased colony formation in soft agar under fluvastatin treatment. Colonies were treated with 20 μmol/L fluvastatin 2× weekly for 14 to 16 days. Bars, mean + SD,  $n = 3$ . \*,  $P < 0.05$  (one-way ANOVA with a Dunnett posttest, comparing all columns vs. vector control column).

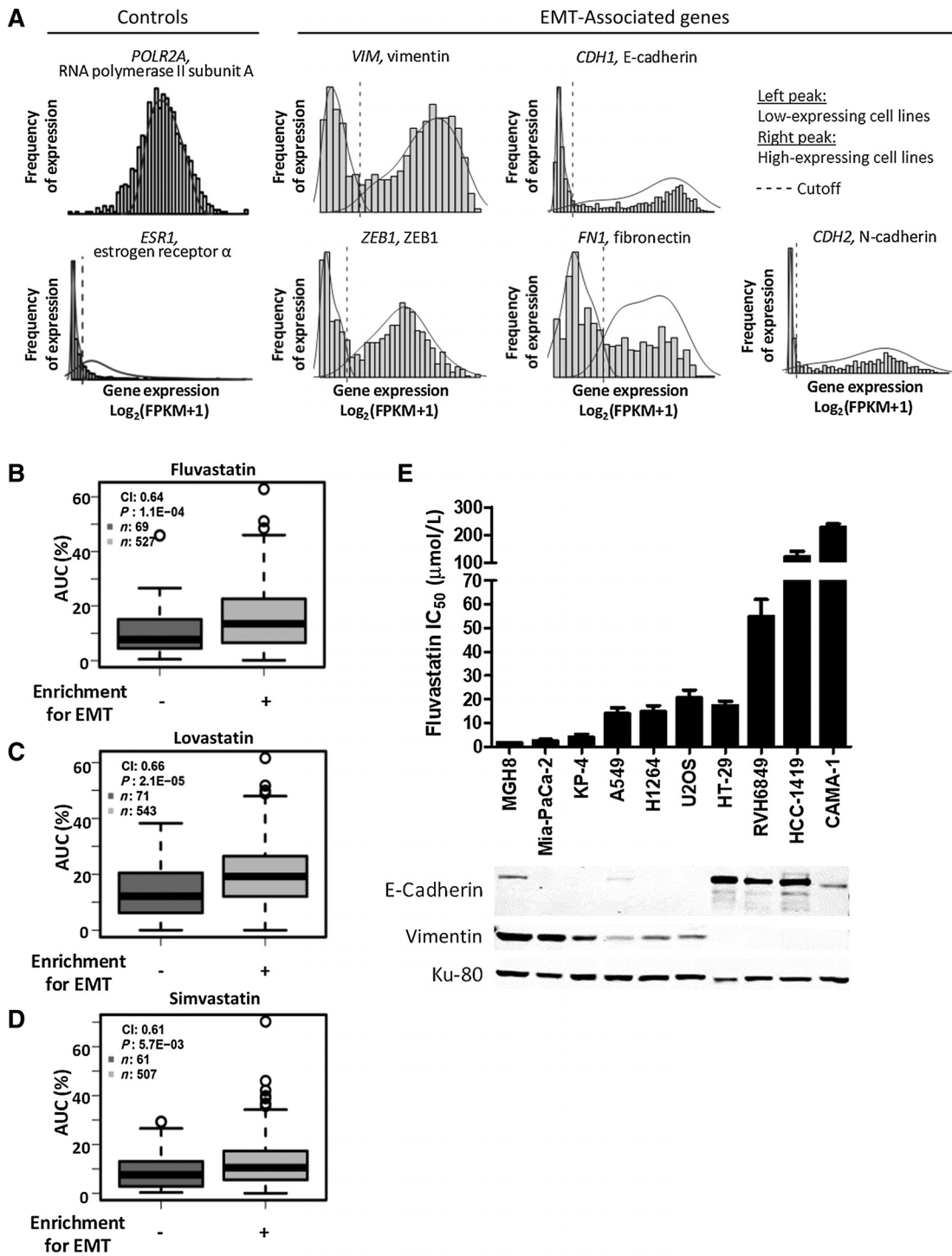


**Figure 5.** Statin sensitivity is associated with cancer cell EMT. **A**, Unimodal (Gaussian) distribution of *POLR2A* and bimodal distribution of *ESR1* (left) are used as controls for gene expression distribution analyses. Bimodal expression of the five EMT-associated genes (right) was used to classify cell lines. Gene expression values are  $\text{log}_2(\text{FPKM}+1)$  with fragments per kilobase of transcript per million mapped reads (FPKM). **B-D**, Sensitivity to three statin family members are significantly associated with cell lines enriched for EMT features. AUC, area under the curve (higher values represent higher drug sensitivity);  $P$  value, Wilcoxon rank sum test, comparing statin response on EMT "enriched" vs. "not-enriched" cell lines;  $n$ , number of cell lines. Of a total of 631 cancer cell lines derived from solid tumors, 596 have been evaluated for sensitivity to fluvastatin, 614 have been evaluated for sensitivity to lovastatin, and 568 have been evaluated for sensitivity to simvastatin. The script and data used for the generation of these figures can be downloaded at <https://github.com/bhklab/StatinEMT>. **E**, Sensitivity to fluvastatin (lower  $\text{IC}_{50}$  values) is positively associated with E-cadherin expression and negatively associated with vimentin expression across a panel of cancer-derived cell lines.

Downloaded from <http://aacrjournals.org/cancerres/article-pdf/78/5/1347/2603890/1347.pdf> by guest on 25 April 2025



Bioconductor package (30), and demonstrated that the EMT-enriched cell lines were associated with significantly higher AUC (more sensitive) to all three statin family members that have been assessed in CTRPv2: fluvastatin (Fig. 5B), lovastatin (Fig. 5C), and simvastatin (Fig. 5D; Wilcoxon rank sum test  $P$ -value  $< 0.001$ ). Thus, cancer cell EMT is associated with sensitivity to multiple statin family members in a large panel of cancer cell lines, across multiple cancer types. As a negative control, we showed that *ESR1* expression levels are not correlated with statin sensitivity (Supplementary Fig. S5D–S5F). Finally, using a panel of 10 cancer-derived cell lines, we showed that fluvastatin  $IC_{50}$  is positively associated with E-cadherin expression and negatively associated with vimentin expression (Fig. 5E), strengthening our conclusion that statin sensitivity is associated with an enrichment of EMT phenotype.

## Discussion

Previously, the increased cancer cell sensitivity to statins was thought to be mediated by inhibiting prenylation of proteins in the RAS superfamily. This model was built on three observations: (i) statins inhibit prenylation of RAS family proteins (8, 11, 12, 17–21); (ii) coadministration of GGPP or FPP with statins reverses the effect on protein prenylation (8, 11, 13, 17–21); and (iii) coadministration of GGPP or FPP can rescue statin kill (8, 13–15, 18–20). However, most epidemiological studies and clinical trials do not support an association between response to statins and RAS mutations (34–39). Additionally, in cell lines that were sensitive to statins, rescuing RAS localization (8, 40) or RAF–MEK–ERK signaling (41) did not decrease statin sensitivity, and intrinsic sensitivity to statin kill was largely independent of RAS function (8, 42). These contradicting data raise the possibility that inhibition of RAS family protein prenylation is not the sole contributor to statin sensitivity, implicating not only an alternative mechanism of statin-induced apoptosis, but also the potential to develop better biomarkers for the identification of patients that will benefit from statin treatment.

We show here that statin-induced cell death can indeed be uncoupled from inhibition of RAS family protein prenylation. First, increased cellular demand for GGPP and FPP for ectopic expression of RAS family proteins requiring prenylation for activity did not always sensitize MCF10A cells to fluvastatin (Fig. 1). Although RAS overexpression led to an increased sensitivity to fluvastatin, this effect was independent from RAS prenylation and localization to the cell membrane (Fig. 2). Instead, RAS induced EMT by upregulating ZEB1, which was the underlying cause of the increased sensitivity to fluvastatin-induced cell death (Figs. 3 and 4). This can, in part, explain why statins have been reported to be more effective in more aggressive (invasive/metastatic) cancer subtypes (2, 3, 42), while mutations in RAS family proteins are poorly associated with statin response (33–38).

Interestingly, when we assayed for the expression profile of a cohort of 11 genes known to be strongly associated with EMT (43), we observed that they followed a bimodal distribution (Supplementary Fig. S5C). Bimodal distribution of *VIM*, *CDH1*, *ZEB1*, *FN1*, or *CDH2* were used as features to classify all solid tumor cell lines in the CCLE (26) into high expression and low expression populations (Fig. 5A). As a comparison, *ESR1* (estrogen receptor  $\alpha$ ) is known to be bimodally expressed in breast cancer (32, 33), which could be used as a classifier of

estrogen receptor-positive and -negative breast tumors in large bioinformatics databases (Supplementary Fig. S5B; ref. 32). CTRPv2 (27–29), we interrogated sensitivity to three statin family members in >500 solid tumor cell lines for any association with an EMT phenotype. Cell lines enriched with EMT features were associated with significantly higher AUC in response to statin treatment (Fig. 5B–D), indicating that they were more sensitive to the antiproliferative effects of statins. Thus, our original observation in the MCF10A model system is expanded to include >20 cancer types and three statin family members, suggesting that the association between EMT and increased sensitivity to statins can be generalized across a broad range of solid tumor cell lines.

Activation of EMT is proposed to be the critical initiating step in metastatic dissemination of late-stage cancers (43). Although it is still debated whether this process is required for metastasis, as opposed to being a phenotype of aggressive/metastatic disease (44, 45), it is nevertheless known to be associated with cell de-differentiation, stem-like properties, and antiapoptotic signaling (46). Importantly, activation of EMT is typically associated with therapeutic resistance (44–46). We show here that activation of EMT increased cell sensitivity to fluvastatin (Fig. 3; Supplementary Fig. S4), consistent with previous reports (47–49). This suggests the intriguing possibility that statins may be used to target disseminated and/or dormant cancer cells (that is, those that presumably have undergone EMT) that are responsible for therapeutic failure and refractory disease. Several epidemiological studies have reported supporting evidence, showing that statin use in breast cancer patients following front-line treatment was associated with better disease-free survival and overall survival (5, 7). Further testing of statins as adjuvant therapeutics in the preclinical and clinical setting is warranted.

It is perhaps tempting to ask which prenylated protein(s), other than the ones selected for testing in this study, is/are responsible for the anticancer effects of statins in the context of EMT. Indeed, we show that coadministration of GGPP or FPP could rescue fluvastatin kill in both HRAS<sup>G12V</sup>- and myr-HRAS<sup>G12V</sup>-overexpressing cells (Fig. 2G–I). However, the two isoprenoids did not rescue to the same extent: GGPP and MVA completely rescued cell death to control levels, but FPP was less effective (Fig. 2G–I). This is reminiscent of previous studies, where GGPP consistently rescued statin effects (8, 11, 13–15, 18–20), while FPP did so less consistently, rescuing completely (11), partially (8, 13, 14, 18), or not at all (15, 18, 21). Nonetheless, the observation that FPP did not rescue as well as GGPP in an HRAS<sup>G12V</sup>-overexpressing system was unexpected, since HRAS prefers FPP over GGPP for prenylation (16). Two explanations are possible for this observation. First, because FPP also acts as the precursor to sterols (1, 10), a portion of the supplemented FPP could be shunted towards cholesterol production, which does not play a role in statin-induced apoptosis (8). However, the observation that MVA consistently rescues statin-induced cell death (8, 11) (Fig. 2G–I) argues against this interpretation. Alternatively, GGPP also functions as the precursor for other isoprenoids such as dolichols and isoprenoid moieties on coenzyme Q (1, 10), and depletion of these larger isoprenoids could be contributing to statin sensitivity. Consistent with this is the observation that cells overexpressing ZEB1 were more sensitive to fluvastatin, but not to inhibition of geranylgeranylation itself through GGTI (Fig. 3G and H). Taken together, our data reinforce the new model presented here that, in the context of cancer cell EMT,

fluvastatin-induced cell death is uncoupled from inhibition of RAS family protein prenylation. Why cells become dependent on the MVA pathway when undergoing EMT, and are therefore sensitive to fluvastatin inhibition, remains to be elucidated and will be an interesting area for future investigation that could lead to the identification of additional biomarkers of fluvastatin-responsive cancers.

### Disclosure of Potential Conflicts of Interest

No potential conflicts of interest were disclosed.

### Authors' Contributions

Conception and design: R. Yu, L.Z. Penn

Development of methodology: R. Yu, B. Haibe-Kains

Acquisition of data (provided animals, acquired and managed patients, provided facilities, etc.): R. Yu, J.E. van Leeuwen, P.J. Mullen, B. Haibe-Kains

Analysis and interpretation of data (e.g., statistical analysis, biostatistics, computational analysis): R. Yu, J. Longo, W. Ba-Alawi, B. Haibe-Kains

Writing, review, and/or revision of the manuscript: R. Yu, J. Longo, J.E. van Leeuwen, W. Ba-Alawi, B. Haibe-Kains, L.Z. Penn

Study supervision: L.Z. Penn

### References

- Goldstein JL, Brown MS. Regulation of the mevalonate pathway. *Nature* 1990;343:425–30.
- Kumar AS, Benz CC, Shim V, Minami CA, Moore DH, Esserman LJ. Estrogen receptor-negative breast cancer is less likely to arise among lipophilic statin users. *Cancer Epidemiol Biomarkers Prev* 2008;17:1028–33.
- Loeb S, Kan D, Helfand BT, Nadler RB, Catalona WJ. Is statin use associated with prostate cancer aggressiveness? *BJU Int* 2010;105:1222–5.
- Nielsen SF, Nordestgaard BG, Bojesen SE. Statin use and reduced cancer-related mortality. *N Engl J Med* 2012;367:1792–802.
- Ahern TP, Pedersen L, Tarp M. Statin prescriptions and breast cancer recurrence risk: a Danish nationwide prospective cohort study. *J Natl Cancer Inst* 2011;103:1461–8.
- Clendening JW, Pandya A, Li Z, Boutros PC, Martirosyan A, Lehner R, et al. Exploiting the mevalonate pathway to distinguish statin-sensitive multiple myeloma. *Blood* 2010;115:4787–97.
- Campbell MJ, Esserman LJ, Zhou Y, Shoemaker M, Lobo M, Borman E, et al. Breast cancer growth prevention by statins. *Cancer Res* 2006;66:8707–14.
- Wong WW, Clendening JW, Martirosyan A, Boutros PC, Bros C, Khosravi F, et al. Determinants of sensitivity to lovastatin-induced apoptosis in multiple myeloma. *Mol Cancer Ther* 2007;6:1886–97.
- Garwood ER, Kumar AS, Baehner FL, Moore DH, Au A, Hylton N, et al. Fluvastatin reduces proliferation and increases apoptosis in women with high grade breast cancer. *Breast Cancer Res Treat* 2010;119:137–44.
- Mullen PJ, Yu R, Longo J, Archer MC, Penn LZ. The interplay between cell signalling and the mevalonate pathway in cancer. *Nat Rev Cancer* 2016;16:718–31.
- Kaneko R, Tsuji N, Asanuma K, Tanabe H, Kobayashi D, Watanabe N. Survivin down-regulation plays a crucial role in 3-hydroxy-3-methylglutaryl coenzyme A reductase inhibitor-induced apoptosis in cancer. *J Biol Chem* 2007;282:19273–81.
- Tsubaki M, Mashimo K, Takeda T, Kino T, Fujita A, Itoh T, et al. Statins inhibited the MIP-1alpha expression via inhibition of Ras/ERK and Ras/Akt pathways in myeloma cells. *Biomed Pharmacother* 2016;78:23–9.
- Finlay GA, Malhowski AJ, Liu Y, Fanburg BL, Kwiatkowski DJ, Toksoz D. Selective inhibition of growth of tuberous sclerosis complex 2 null cells by atorvastatin is associated with impaired Rheb and Rho GTPase function and reduced mTOR/S6 kinase activity. *Cancer Res* 2007;67:9878–86.
- Araki M, Maeda M, Motojima K. Hydrophobic statins induce autophagy and cell death in human rhabdomyosarcoma cells by depleting geranylgeranyl diphosphate. *Eur J Pharmacol* 2012;674:95–103.
- Taylor-Harding B, Orsulic S, Karlan BY, Li AJ. Fluvastatin and cisplatin demonstrate synergistic cytotoxicity in epithelial ovarian cancer cells. *Gynecol Oncol* 2010;119:549–56.
- Berndt N, Hamilton AD, Sebt SM. Targeting protein prenylation for cancer therapy. *Nat Rev Cancer* 2011;11:775–91.
- Tsubaki M, Takeda T, Sakamoto K, Shimaoka H, Fujita A, Itoh T, et al. Bisphosphonates and statins inhibit expression and secretion of MIP-1alpha via suppression of Ras/MEK/ERK/AML-1A and Ras/PI3K/Akt/AML-1A pathways. *Am J Cancer Res* 2015;5:168–79.
- Elsayed M, Kobayashi D, Kubota T, Matsunaga N, Murata R, Yoshizawa Y, et al. Synergistic antiproliferative effects of zoledronic acid and fluvastatin on human pancreatic cancer cell lines: an in vitro study. *Biol Pharm Bull* 2016;39:1238–46.
- Rigoni M, Riganti C, Vitale C, Griggio V, Campia I, Robino M, et al. Simvastatin and downstream inhibitors circumvent constitutive and stromal cell-induced resistance to doxorubicin in IGHV unmutated CLL cells. *Oncotarget* 2015;6:29833–46.
- Moriceau G, Roelofs AJ, Brion R, Redini F, Ebetion FH, Rogers MJ, et al. Synergistic inhibitory effect of apomine and lovastatin on osteosarcoma cell growth. *Cancer* 2012;118:750–60.
- Kusama T, Mukai M, Tatsuta M, Nakamura H, Inoue M. Inhibition of transendothelial migration and invasion of human breast cancer cells by preventing geranylgeranylation of Rho. *Int J Oncol* 2006;29:217–23.
- Soule HD, Maloney TM, Wolman SR, Peterson WD Jr, Brenz R, McGrath CM, et al. Isolation and characterization of a spontaneously immortalized human breast epithelial cell line, MCF-10. *Cancer Res* 1990;50:6075–86.
- Wasylishen AR, Stojanova A, Oliveri S, Rust AC, Schimmer AD, Penn LZ. New model systems provide insights into Myc-induced transformation. *Oncogene* 2011;30:3727–34.
- Haeussler M, Schonig K, Eckert H, Eschstruth A, Mianne J, Renaud JB, et al. Evaluation of off-target and on-target scoring algorithms and integration into the guide RNA selection tool CRISPOR. *Genome Biol* 2016;17:148.
- Sanjana NE, Shalem O, Zhang F. Improved vectors and genome-wide libraries for CRISPR screening. *Nat Methods* 2014;11:783–4.
- Baretina J, Caponigro G, Stransky N, Venkatesan K, Margolin AA, Kim S, et al. The Cancer Cell Line Encyclopedia enables predictive modelling of anticancer drug sensitivity. *Nature* 2012;483:603–7.
- Rees MG, Seashore-Ludlow B, Cheah JH, Adams DJ, Price EV, Gill S, et al. Correlating chemical sensitivity and basal gene expression reveals mechanism of action. *Nat Chem Biol* 2016;12:109–16.

### Acknowledgments

We thank Drs. David Hedley, Senthil Muthuswamy, Catherine O'Brien, Ming Tsao, and Bradley Wouters for providing reagents. We also thank Lindsay Lustig and Aaliya Tamachi for technical assistance, and all members of the Penn lab for helpful discussion and critical review of the manuscript. This work was supported by funding from the Canada Research Chairs Program (to L.Z. Penn; 950-229872), Canadian Institutes of Health Research (to L.Z. Penn; MOP-142263), Terry Fox Research Institute (to L.Z. Penn, B. Haibe-Kains, and W. Ba-Alawi; 1064), CIHR Canada Graduate Scholarship (to R. Yu), Ontario Graduate Scholarship (to J. Longo), and Ontario Student Opportunity Trust Fund (to J.E. van Leeuwen). This work was also supported by the Office of the Assistant Secretary of Defense for Health Affairs, through the Breast Cancer Research Program under Award No. W81XWH-16-1-0068 (to L.Z. Penn). Opinions, interpretations, conclusions and recommendations are those of the author and are not necessarily endorsed by the Department of Defense.

The costs of publication of this article were defrayed in part by the payment of page charges. This article must therefore be hereby marked *advertisement* in accordance with 18 U.S.C. Section 1734 solely to indicate this fact.

Received April 25, 2017; revised October 4, 2017; accepted November 30, 2017; published OnlineFirst December 11, 2017.

28. Seashore-Ludlow B, Rees MG, Cheah JH, Cokol M, Price EV, Coletti ME, et al. Harnessing connectivity in a large-scale small-molecule sensitivity dataset. *Cancer Discov* 2015;5:1210–23.
29. Basu A, Bodycombe NE, Cheah JH, Price EV, Liu K, Schaefer GI, et al. An interactive resource to identify cancer genetic and lineage dependencies targeted by small molecules. *Cell* 2013;154:1151–61.
30. Smirnov P, Safikhani Z, El-Hachem N, Wang D, She A, Olsen C, et al. PharmacGx: an R package for analysis of large pharmacogenomic datasets. *Bioinformatics* 2016;32:1244–6.
31. Wang J, Wen S, Symmans WF, Pusztai L, Coombes KR. The bimodality index: a criterion for discovering and ranking bimodal signatures from cancer gene expression profiling data. *Cancer Inform* 2009;7:199–216.
32. Gendoo DM, Ratanasirigulchai N, Schroder MS, Pare L, Parker JS, Prat A, et al. Genefu: an R/Bioconductor package for computation of gene expression-based signatures in breast cancer. *Bioinformatics* 2016;32:1097–9.
33. Muftah AA, Aleskandarany M, Sonbul SN, Nolan CC, Diez Rodríguez M, Caldas C, et al. Further evidence to support bimodality of oestrogen receptor expression in breast cancer. *Histopathology* 2017;70:456–65.
34. Krens LL, Simkens LH, Baas JM, Koomen ER, Gelderblom H, Punt CJ, et al. Statin use is not associated with improved progression free survival in cetuximab treated KRAS mutant metastatic colorectal cancer patients: results from the CAIRO2 study. *PLoS One* 2014;9:e112201.
35. Lee JE, Baba Y, Ng K, Giovannucci E, Fuchs CS, Ogino S, et al. Statin use and colorectal cancer risk according to molecular subtypes in two large prospective cohort studies. *Cancer Prev Res* 2011;4:1808–15.
36. Baas JM, Krens LL, ten Tije AJ, Erdkamp F, van Wezel T, Morreau H, et al. Safety and efficacy of the addition of simvastatin to cetuximab in previously treated KRAS mutant metastatic colorectal cancer patients. *Invest New Drugs* 2015;33:1242–7.
37. Baas JM, Krens LL, Bos MM, Portielje JE, Batman E, van Wezel T, et al. Safety and efficacy of the addition of simvastatin to panitumumab in previously treated KRAS mutant metastatic colorectal cancer patients. *Anticancer Drugs* 2015;26:872–7.
38. Hong JY, Nam EM, Lee J, Park JO, Lee SC, Song SY, et al. Randomized double-blinded, placebo-controlled phase II trial of simvastatin and gemcitabine in advanced pancreatic cancer patients. *Cancer Chemother Pharmacol* 2014;73:125–30.
39. Ng K, Ogino S, Meyerhardt JA, Chan JA, Chan AT, Niedzwiecki D, et al. Relationship between statin use and colon cancer recurrence and survival: results from CALGB 89803. *J Natl Cancer Inst* 2011;103:1540–51.
40. DeClue JE, Vass WC, Papageorge AG, Lowy DR, Willumsen BM. Inhibition of cell growth by lovastatin is independent of ras function. *Cancer Res* 1991;51:712–7.
41. Wu J, Wong WW, Khosravi F, Minden MD, Penn LZ. Blocking the Raf/MEK/ERK pathway sensitizes acute myelogenous leukemia cells to lovastatin-induced apoptosis. *Cancer Res* 2004;64:6461–8.
42. Goard CA, Chan-Seng-Yue M, Mullen PJ, Quiroga AD, Wasylshen AR, Clendening JW, et al. Identifying molecular features that distinguish fluvastatin-sensitive breast tumor cells. *Breast Cancer Res Treat* 2014;143:301–12.
43. Thiery JP. Epithelial-mesenchymal transitions in tumour progression. *Nat Rev Cancer* 2002;2:442–54.
44. Fischer KR, Durrans A, Lee S, Sheng J, Li F, Wong STC, et al. Epithelial-to-mesenchymal transition is not required for lung metastasis but contributes to chemoresistance. *Nature* 2015;527:472–6.
45. Zheng X, Carstens JL, Kim J, Scheible M, Kaye J, Sugimoto H, et al. Epithelial-to-mesenchymal transition is dispensable for metastasis but induces chemoresistance in pancreatic cancer. *Nature* 2015;527:525–30.
46. Pattabiraman DR, Weinberg RA. Targeting the epithelial-to-mesenchymal transition: the case for differentiation-based therapy. *Cold Spring Harb Symp Quant Biol* 2016;81:11–19.
47. Kang S, Kim ES, Moon A. Simvastatin and lovastatin inhibit breast cell invasion induced by H-Ras. *Oncol Rep* 2009;21:1317–22.
48. Warita K, Warita T, Beckwitt CH, Schurdak ME, Vazquez A, Wells A, et al. Statin-induced mevalonate pathway inhibition attenuates the growth of mesenchymal-like cancer cells that lack functional E-cadherin mediated cell cohesion. *Sci Rep* 2014;4:7593.
49. Fan Z, Jiang H, Wang Z, Qu J. Atorvastatin partially inhibits the epithelial-mesenchymal transition in A549 cells induced by TGF- $\beta$ 1 by attenuating the upregulation of SphK1. *Oncol Rep* 2016;36:1016–22.